J Therm Anal Calorim (2009) 97:173–177
DOI 10.1007/s10973-009-0241-y

Synthesis and thermal decomposition of $SrTi_{1-x}Fe_xO_3$ ($0.0 \leq x \leq 0.1$) powders obtained by the polymeric precursor method

L. F. da Silva · M. I. B. Bernardi · L. J. Q. Maia · G. J. M. Frigo · V. R. Mastelaro

ICTAC2008 Conference

Abstract This work reports on the synthesis of a $SrTi_{1-x}Fe_xO_3$ nanostructured compound ($0.0 \leq x \leq 0.1$) using a modified polymeric precursor method. The effect of the addition of iron on the thermal, structural and morphological properties of the nanoparticles was investigated by FT-IR spectroscopy, X-ray diffraction, and field emission scanning electron microscopy (FE-SEM). A thermogravimetric analysis indicated that the crystallization process preceded by three decomposition steps. Differential thermal analysis experiments showed that decomposition occurred in a broad range of temperatures from 400 to 600 °C. It was observed that iron ions acted as catalysts, promoting rapid organic decomposition and phase formation at a lower temperature than in $SrTiO_3$. Moreover, the addition of iron decreased the crystallite size and increased the lattice parameter of the $SrTi_{1-x}Fe_xO_3$ structure.

Keywords $SrTi_{1-x}Fe_xO_3$ powders · Pechini method · Thermal decomposition · Nanostructured materials

Introduction

Perovskite structured compounds have been studied extensively mainly due to their technological applications, particularly ABO_3 compounds (A = Sr, Ba, Pb, Ca and B = Ti, Zr), which display interesting properties such as photoluminescence [1–3], ferroelectricity [4] and piezoelectricity [5]. These materials have therefore been considered for application as capacitors, varistors, photoelectrodes, ferroelectric memories, gas sensors, etc. With regard to its application as a gas sensor, more recently, highly iron-doped strontium titanate ($SrTiO_3$) has been applied successfully as an oxygen sensor for the control of vehicle emissions [6, 7]. The addition of Fe_2O_3 to the $SrTiO_3$ network, forming $SrTi_{1-x}Fe_xO_3$ (STF) solid solution, has also attracted the interest of researchers because the substitution of titanium by iron atoms, which creates different types of defects due to the difference in the oxidation state of Ti^{4+} and Fe^{3+} [8], contributes to the stabilization of the perovskite phase [9]. Furthermore, the STF system shows a p-type conducting behavior at high temperatures and oxygen partial pressure [10], which renders it a promising material for gas sensor applications.

The conventional method for preparing STF compounds is based on the solid-state reaction of $SrCO_3$, Fe_2O_3 and TiO_2 precursors [6–10]. It is well known that the solid-state reaction requires high temperatures for the sintering process and can produce ceramic powders with chemical inhomogeneity and micrometric particles. It has been observed that the decrease of micro to nanoparticles enhances the property of STF samples [8]. In order to decrease particle sizes to a nanoscale, microsized samples have been subjected to ball milling, which may introduce impurities into them. The synthesis of nanostructured materials by a chemical route appears to be a good alternative to obtain nanostructured powder samples without such inhomogeneities.

In this work, $SrTi_{1-x}Fe_xO_3$ (STF) solid solution was obtained by a modified polymeric precursor method. This method offers the advantages of good stoichiometric control, easy reproducibility and nanosized particles [11]. The

L. F. da Silva · M. I. B. Bernardi · G. J. M. Frigo · V. R. Mastelaro (✉)
Instituto de Física de São Carlos – USP, São Carlos, SP, Brazil
e-mail: valmor@ifsc.usp.br

L. J. Q. Maia
Instituto de Física, Universidade Federal de Goiás – UFG, Goiânia, GO, Brazil

effect of the addition of iron on the thermal and structural properties of $SrTiO_3$ powders was investigated by thermogravimetric analysis (TG), differential thermal analysis (DTA), X-ray diffraction (XRD) measurements and Fourier transform infrared (FT-IR) spectroscopy. In addition, the morphology of the nanoparticles was examined under a field emission scanning electron microscope (FE-SEM).

Experimental

Crystalline $SrTi_{1-x}Fe_xO_3$ powders with $x = 0.0$, 0.05 and 0.10 were prepared by a modified Pechini method [12, 13]. The following reagents were used as precursor materials during the synthesis: strontium carbonate ($SrCO_3$—Merck, 99.9%), titanium (IV) isopropoxide ($Ti[OCH(CH_3)_2]_4$—Alfa Aesar, 97%), and iron (III) nitrate ($Fe(NO_3)_3.9H_2O$—Sigma, 98%).

First, the citric acid (CA) and iron nitrate were dissolved in distilled water (at room temperature) under constant agitation. After complete dissolution, the temperature of the solution was raised to 80 °C and the $SrCO_3$ was added slowly to the aqueous solution until it became transparent. Ethylene glycol (EG) was then added to this solution, which was heated to 150 °C. The molar ratio of the cations (Sr + Fe) and citric acid (CA) was 4:1. The titanium citrate solution was then prepared in a separate container. The citrate was formed by dissolving citric acid (CA) and titanium isopropoxide in distilled water at 70 °C. The CA:Ti molar ratio was 4:1. After complete homogenization of the CA in the citrate solution, the EG was added to the solution at a mass ratio of 40:60. The Sr-Fe–Ti resin was prepared by mixing strontium-iron and titanium solutions, maintaining a molar ratio of 1:1 (Sr:Ti + Fe). This procedure yielded a colorless resin. The temperature of the solution was then raised to 150 °C to eliminate water, causing the solution to become viscous. After that, the solution was heat-treated at 300 °C for 8 h at a heating rate of 10 °C min^{-1} to eliminate any remaining organic species. The powders obtained by this process were called the "precursor". These precursor powders were calcined at 700 °C for 1 h (twice) in an electric furnace in an air atmosphere.

Thermal studies of precursor powders were performed by thermogravimetry (Netzsch, TG 209) and differential thermal analysis (TA Instruments, DSC 2920). These measurements were carried out from room temperature to 800 °C under a synthetic air atmosphere at a heating rate of 10 °C min^{-1}, using the Al_2O_3 compound as reference. The crystalline STF powders were characterized structurally by X-ray diffraction (XRD) measurements in a 2θ range from 20 to 80° with a step of 0.020°, at a scanning speed of 2°min^{-1}, using a CuKα radiation (Rigaku, Rotaflex RU200B). The infrared bands were studied in the 2000–400 cm^{-1} range using a FT-IR spectrometer (PerkinElmer, Spectrum GX). Lastly, a microstructural analysis was carried out using a field emission scanning electron microscope (FE-SEM, Zeiss SUPRA35) operating at 5.0 kV.

Results and discussion

Thermal analysis

Figure 1 shows the thermogravimetric curve (TG) and its derivative (DTG) of the precursor powders containing different iron contents. Figure 2 illustrates the DTA curves of the same powders analyzed by TG technique. Note the presence of four peaks in the DTG curves of all the samples, one at around 100 °C, which was attributed to the elimination of water, and three peaks between 450 and 700 °C, ascribed to the decomposition of organic species [14]. These peaks occurred at 500, 620 and 700 °C in the $SrTiO_3$ sample, at 460, 590 and 630 °C in the $SrTi_{0.95}Fe_{0.05}O_3$ compound, and at 450, 520 and 580 °C in the $SrTi_{0.90}Fe_{0.10}O_3$ sample. Table 1 presents the mass loss data resulting from the TG measurements. A dehydration-related mass loss of 8–10% was observed between 25 and 250 °C, of 34–38% between 250 and 550 °C, and of

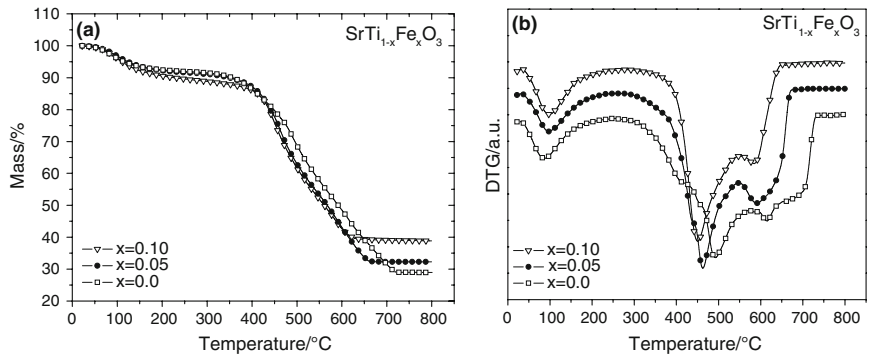

Fig. 1 **a** TG curves and **b** DTG curves of the $SrTi_{1-x}Fe_xO_3$ amorphous precursors

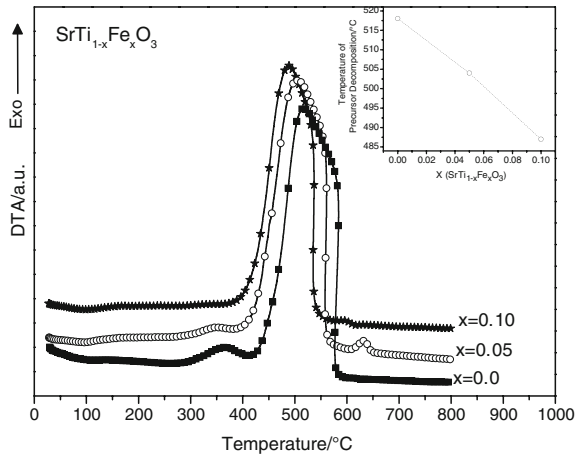

Fig. 2 DTA curves of the $SrTi_{1-x}Fe_xO_3$ amorphous precursors. The inset shows the variation of the decomposition temperature of the precursor with composition

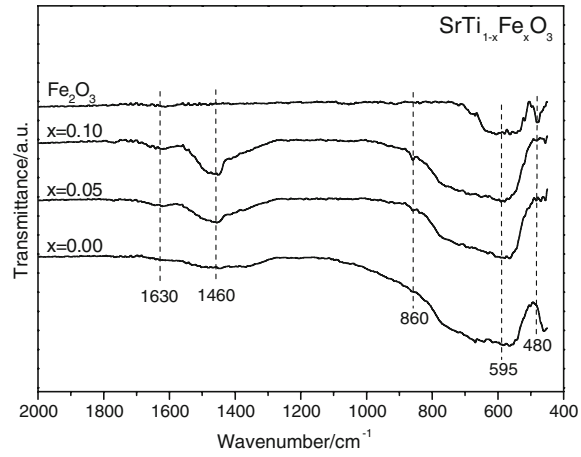

Fig. 3 FT-IR spectra of crystalline $SrTi_{1-x}Fe_xO_3$ powders

Table 1 Thermal analysis data of precursor powders

X	Dehydration/%	Oxidation decomposition/%	Decomposition of residual CO_2 and phase formation/%
	25–250 °C	250–550 °C	550–720 °C
0.0	8	34	29
0.05	8	38	21
0.10	10	38	13

29–13% between 550 and 720 °C. A considerable reduction in mass loss was observed between 550 and 720 °C in response to the increase in iron content.

On the other hand, the DTA measurements (Fig. 2) revealed a broad exothermic peak between 400 and 600 °C. An analysis of the maximum temperature of this peak (inset of Fig. 2), indicated that it decreased linearly as the iron content increased, starting from about 518 °C ($x = 0.0$) up to 487 °C ($x = 0.10$). This behavior was probably due to the changes in the polymerization or pyrolysis process, which can be influenced by the catalytic effect caused by the incorporation iron into the $SrTiO_3$ network. Iron undoubtedly acts as a catalyst, promoting rapid organic decomposition at low temperatures. Souza et al. [15] have reported similar findings in $Sr_{1-x}Mg_xTiO_3$ powders obtained by the polymeric precursor method. The presence of two additional peaks at 630 and 600 °C in the $x = 0.05$ and 0.10 samples, respectively, could be related to the crystallization temperature of these compounds.

Structural analysis

The FT-IR spectra of the crystalline STF powders and the Fe_2O_3 (hematite) reference compound are presented in Fig. 3. The position of the peaks is identified by a dashed line. An analysis of the spectra showed the presence of a band at 1630 cm^{-1} related to the COO stretching mode for a unidentate complex [16]. On the other hand, although the thermogravimetric measurements indicated a lower temperature for carbonate elimination (see Fig. 1), the IR spectrum still indicated the presence of characteristics bands of CO_3^{-2} carbonate groups at 1460 and 860 cm^{-1}, even after heating to 700 °C [17]. The broad band at 595 cm^{-1} corresponds to Ti–O vibrations, while the band at 480 cm^{-1} is associated with FeO_6 octahedron vibration [18, 19]. As it can be seen, the latter band became more pronounced as the iron content increased.

Figure 4 shows the XRD patterns of crystalline $SrTi_{1-x}Fe_xO_3$ ($x = 0.0$, 0.05 and 0.10) powders calcined at 700 °C for 1 h. All the peaks were attributed to the perovskite structure of $SrTiO_3$ phase (JCPDS:35-0734). No evidence of a secondary phase was found. The average crystallite size was calculated from the full width at half

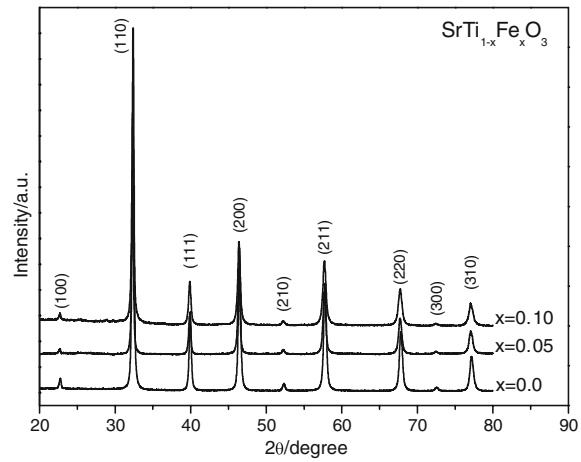

Fig. 4 X-ray diffraction patterns of the crystalline $SrTi_{1-x}Fe_xO_3$ powders

Table 2 Crystallite average size and lattice parameter of the $SrTi_{1-x}Fe_xO_3$ powders

X	Crystallite size (±1 nm)	Lattice parameter ($\pm 1.10^{-3}$ Å)
0.0	36	3.909
0.05	37	3.912
0.10	28	3.920

maximum (FWHM) of the X-ray diffraction lines, using Scherrer's equation [20]. The (110) diffraction peak was used to determine the crystallite size and lattice parameters. Table 2 shows the average crystallite size and the lattice parameters for different iron compositions. Clearly, the crystallite size decreased in response to the substitution of Ti with Fe ions. This behavior can be explained by the role of iron as a catalyst in organic decomposition and by the fact that the crystallization process occurred at a lower temperature than it did for $SrTiO_3$ phase. During the decomposition process, iron ions nucleate the phase while simultaneously forming crystallites, but the diffusion process did not occur due to the low temperature. As the iron content increased, the nucleation rate increased, giving rise to additional smaller crystallite sizes.

The lattice parameter was also found to increase along with the increase in iron content. Vračar et al. [21] reported a similar result for STF powders obtained by solid state reaction in a reduced atmosphere. If one considers that Ti^{4+} is replaced by Fe^{3+} ions, this behavior can be attributed to a difference in the ionic radius of Ti^{4+} (0.605 Å) and Fe^{3+} (0.645 Å). Preliminary results (not shown here) of the oxidation state of iron determined by the XANES (X-ray absorption near edge spectroscopy) technique indicated that the iron ions were predominantly in a Fe^{3+} oxidation state.

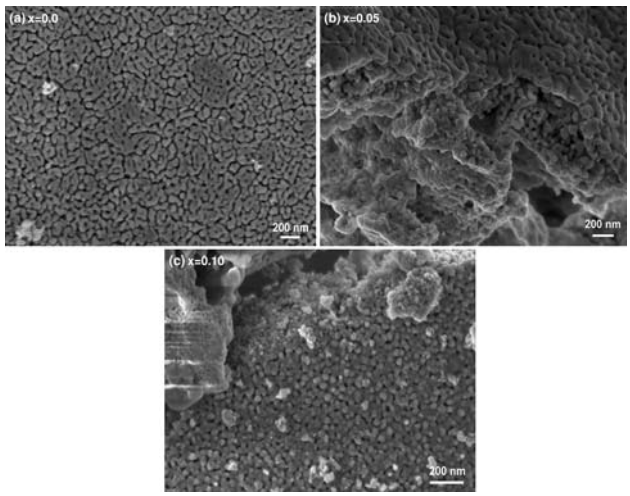

Fig. 5 FE-SEM micrographs of crystalline $SrTi_{1-x}Fe_xO_3$ powders. **a** $x = 0.0$, **b** $x = 0.05$, and **c** $x = 0.10$

Morphology

Figure 5 shows an image of crystalline STF powders with different iron contents. No significant modification was observed in the grain morphology due to the increase in iron content. This figure shows a considerable agglomeration of nanoparticles, independently of the sample's composition. The formation of such agglomerates is probably due to the excessive heat released during the burnout of organic residues (exothermic reaction between 400 and 600 °C depicted in Fig. 1), which promotes partial sintering of the nanoparticles [22].

Conclusions

$SrTi_{1-x}Fe_xO_3$ nanoparticles with $x = 0.0$, 0.05 and 0.01 were successfully synthesized for the first time by a modified polymeric precursor method. The organic decomposition and crystalline phase formation were monitored using the TG and DTA techniques. The analysis of TG curves indicated that the phase formation was preceded by three organic decomposition steps. The DTA curves, which showed a broad peak located between 400 and 600 °C, indicated the occurrence of organic decomposition. The increase in iron content caused a decline in the maximum temperature of the decomposition peak. In fact, iron ions act as a catalyst, promoting more efficient organic decomposition and phase formation at a lower temperature than that required for nondoped $SrTiO_3$. Furthermore, the addition of iron was found to decrease the crystallite size due to low organic decomposition, and to increase the lattice parameter of the STF structure because iron ions have a larger ionic radius than titanium. No evident modification was observed in the morphology of the nanoparticles in response to the increase in iron content.

Acknowledgements The authors are indebted to Prof. Elson Longo for the use of the FE-SEM facility. We also gratefully acknowledge the Brazilian financing agencies FAPESP and CNPq for their financial support.

References

1. Bouma B, Blasse G. Dependence of luminescence of titanates on their crystal structure. J Phys Chem Solids. 1995;56:261–5.
2. Lazaro SD, Milanez J, de Figueiredo AT, Longo VM, Mastelaro VR, de Vicente FS, et al. Relation between photoluminescence emission and local order-disorder in the $CaTiO_3$ lattice modifier. Appl Phys Lett. 2007;90:111904.
3. Sahoo T, Pradhan GK, Rath MK, Pandey B, Verma HC, Nandy S, et al. Characterization and photoluminescence studies on hydrothermally synthesized Mn-doped barium titanate nano powders. Mater Lett. 2007;61:4821–3.
4. Choudhury PR, Krupanidhi SB. Constrained ferroelectricity in BaTiO/BaZrO superlattices. Appl Phys Lett. 2008;92:102903.

5. Luo Y, Szafraniak I, Nagarajan V, Wehrspohn RB, Steinhart M, Wendorff JH, et al. Ferroelectric lead zirconate titanate and barium titanate nanotubes. Integr Ferroelectr. 2003;59:1513–20.
6. Moos R, Menesklou W, Schreiner HJ, Härdtl KH. Materials for temperature independent resistive oxygen sensors for combustion exhaust gas control. Sens Actuators B. 2000;67:178–83.
7. Rothschild A, Tuller HL. Gas sensors: new materials and processing approaches. J Eletroceram. 2006;17:1005–12.
8. Rothschild A, Menesklou W, Tuller HL, Ivers-Tiffée E. Electronic structure, defect chemistry, and transport properties of $SrTi_{1-x}Fe_xO_3$-y solid solutions. Chem Mater. 2006;18:3651–9.
9. Brixner LH. Preparation and properties of the $SrTi_{1-x}Fe_xO_{3-x/2}$ empty set x/2 system. Mater Res Bull. 1968;3:299–308.
10. Meuffels P. Propane gas sensing with high-density $SrTi_{0.6}Fe_{0.4}O_{(3-\delta)}$ ceramics evaluated by thermogravimetric analysis. J Eur Ceram Soc. 2007;27:285–90.
11. Cushing BL, Kolesnichenko VL, O′Connor CJ. Recent advances in the liquid-phase syntheses of inorganic nanoparticles. Chem Rev. 2004;104:3893–946.
12. Mesquita A, Bernardi MIB, Maia LJQ, Mastelaro VR. Synthesis and characterization of $Pb_{1-x}La_xTiO_3$ nanocrystalline powders. J Therm Anal Calorim. 2007;87:747–51.
13. da Silva RS, Bernardi MIB, Hernandes AC. Synthesis of non-agglomerated $Ba_{0.77}Ca_{0.23}TiO_3$ nanopowders by a modified polymeric precursor method. J Sol Gel Sci Technol. 2007; 42:173–9.
14. Camargo ER, Longo E, Leite ER, Kakihana M. Qualitative measurement of residual carbon in wet-chemically synthesized powders. Ceram Int. 2004;30:2235–9.
15. de Souza MAF, Candeia RA, Souza SC, Chaves AC, Lima SJG, Longo E, et al. Synthesis and characterization of $Sr_{1-x}Mg_xTiO_3$ obtained by the polymeric precursor method. Mater Lett. 2005;59:549–53.
16. Mao C, Dong X, Seng T, Wang G, Chen S. Formation and control of mechanism for the preparation of ultra-fine barium strontium titanate powders by the citrate precursor method. Mater Res Bull. 2007;42:1602–10.
17. Kakihana M, Okubo T, Arima M, Nakamura Y, Yashima M, Yoshimura M. Polymerized complex route to the synthesis of pure $SrTiO_3$ at reduced temperatures: implication for formation of Sr-Ti heterometallic citric acid complex. J Sol Gel Sci Technol. 1998;12:95–109.
18. Silva MRS, Soledade LEB, Lima SJG, Longo E, Souza AG, Santos IMG. Influence of processing conditions on the thermal decomposition of $SrTiO_3$ precursors. J Therm Anal Calorim. 2007;87:731–5.
19. Wang X, Gao LS, Zheng HG. Fabrication and electrochemical properties of alpha-Fe_2O_3 nanoparticles. J Cryst Growth. 2004;269:489–92.
20. Klug HP, Alexander LE. X-ray diffraction procedures for polycrystalline and amorphous materials. USA: Wiley; 1954. p. 410.
21. Vračar M, Kuzmin A, Merkle R, Purans J, Kotomin EA, Maier J, et al. Jahn-Teller distortion around Fe^{4+} $Sr(Fe_xTi_{1-x})O_{3-\delta}$ from X-ray absorption spectroscopy, X-ray diffraction, and vibrational spectroscopy. Phys Rev B. 2007;76:174107.
22. Leite ER, Varela JA, Longo E, Paskocimas CA. Influence of polymerization on the synthesis of $SrTiO_3$. Part II. Particle and agglomerate morphologies. Ceram Int. 1995;21:153–8.